Title
Mucin Covalently Bonded to Microfibers Improves the Patency of Vascular Grafts

Journal
Tissue Engineering Part A, 20(1-2)

ISSN
1937-3341

Authors
Janairo, Randall Raphael R
Zhu, YiQian
Chen, Timothy
et al.

Publication Date
2014

DOI
10.1089/ten.tea.2013.0060

Peer reviewed

TISSUE ENGINEERING: Part A
Volume 20, Numbers 1 and 2, 2014

DOI: 10.1089/ten.tea.2013.0060

Mucin Covalently Bonded to Microfibers Improves the Patency of Vascular Grafts

Randall Raphael R. Janairo, PhD,[1,2] YiQian Zhu, PhD,[1,2] Timothy Chen, BS,[1] and Song Li, PhD[1,2]

Due to high incidence of vascular bypass procedures, an unmet need for suitable vessel replacements exists, especially for small-diameter (< 6 mm) vascular grafts. Here, we developed a novel, bilayered, synthetic vascular graft of 1-mm diameter that consisted of a microfibrous luminal layer and a nanofibrous outer layer, which was tailored to possess the same mechanical property as native arteries. We then chemically modified the scaffold with mucin, a glycoprotein lubricant on the surface of epithelial tissues, by either passive adsorption or covalent bonding using the di-amino-poly(ethylene glycol) linker to microfibers. Under static and physiological flow conditions, conjugated mucin was more stable than adsorbed mucin on the surfaces. Mucin could slightly inhibit blood clotting, and mucin coating suppressed platelet adhesion on microfibrous scaffolds. In the rat common carotid artery anastomosis model, grafts with conjugated mucin, but not adsorbed mucin, exhibited excellent patency and higher cell infiltration into the graft walls. Mucin, which can be easily obtained from autologous sources, offers a novel method for improving the hemocompatibility and surface lubrication of vascular grafts and many other implants.

Introduction

Currently, over a half million bypass procedures are performed annually to treat vascular diseases in the United States. An unmet need is the suitable small-diameter vascular graft with patency that can match or outperform autologous grafts. An ideal vascular graft should have characteristics that include antithrombogenicity, resistance to rejection, mechanical compliance similar to native vessels, and capability of self-remodeling. Researchers have attempted to address these ideal properties by developing tissue-engineered cellular vessels using vascular cells[1–4] as well as bone marrow cells. [5–7] Cellular grafts, although successful in exhibiting many of the same properties as autologous grafts, need a long period to fabricate and require significant amount of effort for storage, shipping, and handling. To address this shortcoming, research has employed the decellularized native matrix as well as modified synthetic materials to develop vascular replacements.[8–14] Recently, many research groups have utilized electrospinning to produce fibrous scaffolds for vascular regeneration.[7,12,15–19] These scaffolds consist of fibers that mimic the porous micro- and nanostructure of collagen and elastin fibers, the major native extracellular matrix components in the blood vessel wall.

To maintain the patency of vascular grafts, the luminal surface must be made antithrombogenic, either by cell seeding or surface modification. Heparin, a highly sulfated glycosaminoglycan (GAG), has been used extensively in vascular therapies because of its strong anticoagulant ability. It has been shown to prevent thrombosis on synthetic surfaces and decellularized xenogeneic tissue.[13,20–24] The endothelial cell (EC) monolayer, the natural barrier between blood and tissue, exhibits a glycocalyx layer on its surface. Endothelial glycocalyx is a highly negatively charged coating predominately composed of glycoproteins and proteoglycans, including those containing heparin sulfate GAGs.[25,26] This carbohydrate-rich layer has been shown to be a significant factor in the ability of ECs to prevent nonspecific protein and cell adhesion on the monolayer surface.[26–28] Thus, one potential solution to preventing thrombus formation, subsequent occlusion, and graft failure is to modify their surfaces so that they mimic this passively protective coating.

To accomplish such a modification, inspiration can be drawn from other protective surface coatings in the body. For instance, epithelial cells in naturally harsh environments, such as the gastrointestinal tract, respiratory system, and urinary tract, rely on large, negatively charged, heavily glycosylated proteins known as mucins for protection and selective transport.[29] These glycoproteins have molecular weights ranging from 0.5 to 20 MDa and can be found in a secreted form (as in saliva or mucus) or bound to cell membranes. The three-dimensional configuration of mucin is likened to a bottle brush, with the protein core handle consisting of a vast number of tandem repeats comprising serine, threonine, and proline, to which numerous varieties of

[1]Department of Bioengineering, University of California, Berkeley, California.
[2]University of California Berkeley–University of California San Francisco Graduate Program in Bioengineering, Berkeley and San Francisco, California.

0-linked and *N*-linked oligosaccharides attach and branch out to form the brush.[30]

Because of its structure, mucin increases the surface hydrophilicity of epithelial tissue and suppresses nonspecific plasma protein adsorption and nonspecific cell adhesion.[31] Mucin has been shown to increase hydrophilicity of silicon- and poly(ethylene terephthalate)-based biomaterials.[32,33] Furthermore, mucin has been shown to suppress bacterial adhesion, as well as neutrophil adhesion and activity–events that could lead to fouling and surface thrombosis.[34–36]

Despite this recent progress, however, it is yet to be shown how well mucin can protect synthetic biomaterials *in vivo*, especially at the interface of blood and vascular grafts. Here, we developed a novel, bilayered, electrospun micro- and nanofibrous scaffold to mimic the mechanical strength of native vessels, and investigated the effects of mucin modification on vascular graft performance *in vivo*.

Materials and Methods

Electrospinning of bilayered, micro-/nanofibrous vascular graft scaffold

Poly(L-lactide) (PLLA) (1.09 dL/g inherent viscosity; Lactel Absorbable Polymers) was dissolved in 1,1,1,3,3-hexafluoro-2-propanol (HFIP) by means of sonication for 30 min or until all of the PLLA crystals were completely dissolved, resulting in 19% (w/v) solution. A second polymer blend solution consisting of 10% (w/v) poly(L-lactide-co-caprolactone-co-glycolide) (PLCG) (Sigma-Aldrich) and 5% poly(ε-caprolactone) (PCL) (Sigma-Aldrich) in HFIP (henceforth referred to as the PLCG + PCL solution) was similarly prepared through sonication. Electrospinning was done as previously described,[12] with modifications made to spin the PLLA and PLCG + PCL solutions consecutively onto the same collecting mandrel. Briefly, a voltage of 12 kilovolts (kV) was applied through a high voltage generator (Gamma High Voltage) to a spinneret that was aimed at a grounded, rotating, stainless steel mandrel (1 mm diameter; 150 revolutions/min). Electrospinning of the PLLA solution was performed first and continued until the scaffold wall thickness reached ~50 μm. Electrospinning of the PLCG + PCL solution was started immediately after, onto the same collecting mandrel and continued until the total scaffold wall thickness reached ~100 μm. The resulting scaffold was then removed from the mandrel and placed into a vacuum desiccator for 24 h to remove any residual HFIP. Bulk scaffold and fiber quality and dimensions were inspected using a Hitachi TM-1000 Scanning Electron Microscope (SEM). The bulk scaffold was cut into 7-mm length segments, sterilized in 70% ethanol under germicidal ultraviolet light for 30 min, and washed five times with sterile, deionized water.

Chemical modification of bilayered electrospun vascular graft scaffold

Mucin modification of electrospun scaffolds was accomplished in two ways: (1) passive adsorption by submersing and rotating in 0.1% (w/v) solution of bovine submaxillary mucin (BSM, henceforth referred to as mucin) (Sigma-Aldrich) in 2× phosphate-buffered saline (PBS); and (2) conjugation using 1-ethyl-3-(3 dimethylaminopropyl) carbodiimide hydrochloride (EDC) and N-hydroxysulfosuccinimide (sulfo-NHS) (Pierce Biotechnology) with di-amino-poly(ethylene glycol) (PEG) as a linker.[37] In addition to untreated control grafts, a control group of scaffolds was also PEGylated, using EDC and sulfo-NHS to conjugate PEG only to the electrospun fibers.

Alcian blue binding assay for mucin detection

The presence of mucin on scaffolds was verified by means of Alcian blue binding assay (Sigma-Aldrich) as described previously.[38] Briefly, untreated, PEGylated, mucin-adsorbed (MUC), and mucin-conjugated (PEG-MUC) scaffolds were placed in 0.00015% Alcian blue solution in 7% acetic acid for 30 min at room temperature. The solution for each sample was then extracted, placed in fresh centrifuge tubes, and centrifuged at 10,000 rpm for 5 min. The absorbance of each resulting supernatant was measured at 600 nm using a spectrophotometer (Model 550; BioRad). The amount of dye bound to each treated scaffold was taken as the difference between the absorbance of their supernatant and that of the untreated scaffold and thus reported as ΔAbsorbance. A higher ΔAbsorbance correlated to more mucin on the scaffold.

Stability of mucin modifications under flow condition

PEG-MUC and MUC PLLA microfibrous membranes, as well as untreated and PEGylated controls were immobilized onto one plate of a custom-made, parallel-plate, laminar flow chamber. They were then subject to 24 dynes/cm^2 shear stress produced by flow of PBS for 48 h. The flow chambers were kept in a humidified incubator at 37°C and supplemented with 5% CO_2 throughout the entire flow duration. After the 48-h flow period, relative mucin amounts were detected using the Alcian blue binding assay. These readings were compared to preflow readings, as well as readings taken for static controls at 0 and 48 h.

Effect of mucin solution on blood coagulation time in vitro

The effect of mucin solution on blood coagulation time was tested *in vitro* using modified methods previously described.[39] Briefly, microhematocrit glass capillaries (BD Biosciences) were loaded by means of capillary action with 2.5 μL of different concentrations of mucin, di-amino-PEG, and heparin salt (Sigma-Aldrich) solutions in PBS. Immediately before sacrifice, blood was collected into each solution-loaded capillary tube from the punctured carotid artery of athymic rats by placing the loaded opening of the tube directly adjacent to the puncture site. Enough blood was drawn into the tube such that the final volume in each capillary was 25 μL, as measured by premade markings on the side of each capillary. The chronometer was started at the time of contact between the blood and capillary tube. Immediately after blood draw, the tubes were rotated slowly to allow the blood to flow within a 45-mm length marked on each tube. Time was stopped and recorded once the blood stopped flowing within the capillary tube.

Platelet adhesion assay using whole blood

Whole rat blood was drawn from the athymic rat heart immediately before sacrifice into collection tubes containing

the ACD Solution A (BD Biosciences) to prevent coagulation (9:1 blood:anticoagulant). Untreated, PEGylated, PEG-MUC, and MUC PLLA microfibrous membranes of equal dimensions (nine per experimental group) were immersed in equal amounts of blood and kept in 37°C for 2 h. Samples were then washed and analyzed through SEM and immunofluorescence staining using the anti-rat CD41 antibody (Santa Cruz Biotechnology, Inc.). Positive immunofluorescent antibody staining was tallied for each treatment sample (9 per experimental group) and compared. Platelets on the scaffolds were imaged using a Hitachi TM-1000 SEM.

In vivo *anastomosis model*

All procedures involving animals were approved by the Institutional Review Board Service and Institutional Animal Care and Use Committee at the University of California, San Francisco and the Research Administration and Compliance Office and Animal Care and Use Committee at the University of California, Berkeley. The number of animals used for our *in vivo* assessment was estimated based on previous work[7,12] and recommendations for preclinical studies of vascular intervention.[40]

Adult female athymic rats (8 weeks old, 200 ± 20 g, eight per experimental group) were anesthetized with 2.0% isoflurane then placed in the supine position. The left common carotid artery (CCA) was isolated, exposed, and ligated at 2 points ~8 mm apart, between which the artery segment was dissected. An untreated, PEGylated, PEG-MUC, or MUC vascular graft (8 mm in length and 1 mm in inner diameter) was subsequently sutured end-to-end to the dissected CCA and blood flow was reestablished. No heparin or other anticoagulant was used at any time during these animal studies. After 1 month postoperative procedure, the rats were euthanized by means of CO_2 asphyxiation followed by bilateral thoracotomy, and the vascular grafts were explanted and washed with saline to remove remaining blood. Before explantation, the patency of the grafts was determined. Unobstructed blood flow through the graft was confirmed by instantaneous redistension of the forcibly collapsed distal CCA. This method was verified by Doppler Ultrasound measurement of the flow through the patent grafts. The patency was further confirmed by the histological analysis of the cross sections.

Mechanical testing

Freshly explanted native rat common carotid arteries, preimplanted grafts, and freshly explanted vascular grafts were cut so that 2-mm-long segments could be mounted onto and uniaxially loaded by an Instron mechanical testing machine. The stress–strain curve was obtained for each sample using accompanying Bluehill software. The elastic modulus was calculated from the linear portion of the stress–strain curve acquired for each graft.

Histological analysis

Samples were cryopreserved at −20°C in the Optimal Cutting Temperature (OCT) compound (TissueTek) and subsequently cryosectioned at 10-μm thickness in the cross-sectional plane of the grafts. Immunohistochemical staining was performed to analyze the presence of ECs using the CD31 antibody (BD Biosciences) and smooth muscle cells (SMCs) using the smooth muscle-myosin heavy chain (SM-MHC) antibody (Santa Cruz Biotechnology), as well as collagen and elastin (through Verhoeff staining) and the proliferation marker, Ki67 (Abcam) in the tissue sections. The inflammatory response was assessed by immunofluorescent staining for macrophage populations using the CD68 and CD163 antibodies (Serotec), as well as the CCR7 antibody (Novus Biologicals). Hematoxylin and eosin (H&E) and DAPI nuclear stains were also performed to visualize the cell presence within the graft sections. Images of all aforementioned stains were captured with a Zeiss Axioskop 2 MOT microscope.

Statistical analysis

Quantitative data were calculated as the mean ± standard deviation, where applicable. For comparison between the two groups, a *t*-test was performed. Analysis of variance (ANOVA) was used when comparing the means of three or more groups. When ANOVA revealed a statistical difference, *post hoc* pairwise comparisons were accomplished using the Holm's *t*-test. A *p*-value of less than 0.05 was considered statistically significant.

Results

Electrospinning of bilayered fibrous grafts that mimicked native matrix fiber structure and mechanical strength

We successfully made nonwoven, micro-/nanofibrous, bilayered conduits that were suitable for being used as vascular graft scaffolds (Fig. 1A). Our design incorporated two different polymer solutions—PLLA for the luminal layer and PLCG + PCL for the outer layer. The electrospun products exhibited a structure similar to the native matrix, marked by the fiber morphology and porosity (Fig. 1B, C). The average diameter of the PLLA fibers (Fig. 1B) and PLCG + PCL fibers (Fig. 1C) was ~1.5 μm and 800 nm, respectively. PLLA was chosen for the luminal layer because of its easily customizable and reproducible electrospun products, as well as its well-characterized and highly consistent chemical modification method.[12,37,41] PLCG + PCL was utilized to make the outer layer because of its mechanical properties. The scaffolds containing PLCG + PCL exhibited elastic moduli about three to four times as great as PLLA scaffolds alone, which on average exhibited an elastic modulus of 3.5 MPa.[12] Since the average elastic modulus of the native CCA was 12.6 ± 2.2 MPa, PLCG + PCL was the ideal choice for the mechanically supportive outer layer of our graft design. The utilization of PLCG + PCL as such resulted in a scaffold that matched the stress–strain behavior of the athymic rat CCA (Fig. 1D) and average elastic modulus (Fig. 1E). The average elastic modulus of the bilayered electrospun graft was 12.8 ± 2.5 MPa.

Mucin modification of bilayered electrospun vascular graft scaffolds

The conjugation scheme is shown in Figure 2A. Successful mucin modification was verified using the Alcian blue binding assay, which resulted in a visual color change (Fig. 2B), as well as a positive ΔAbsorbance reading at 600 nm

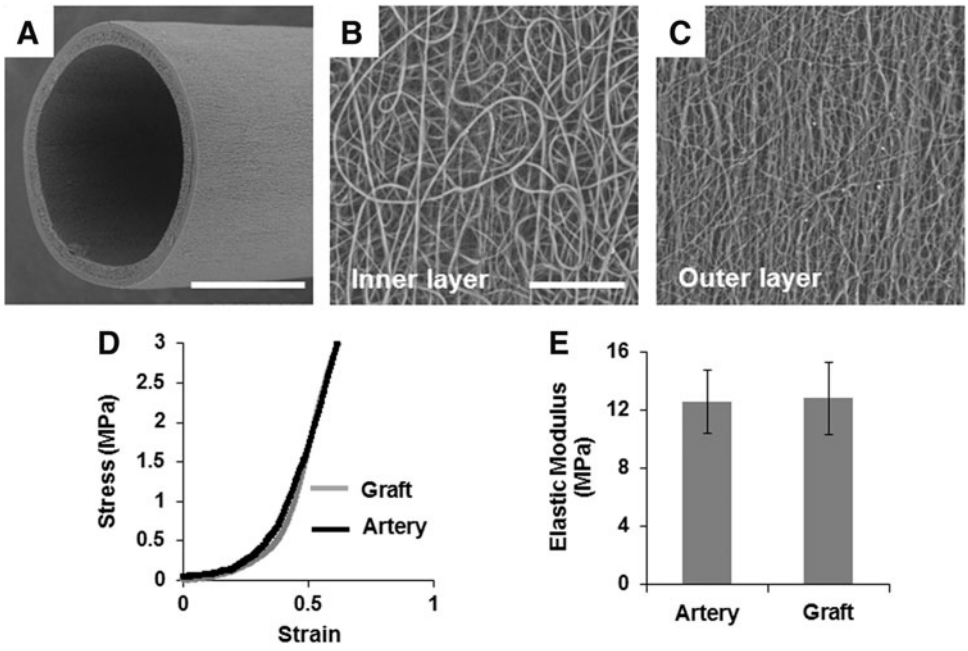

FIG. 1. Structure and mechanical properties of bilayered electrospun vascular grafts. **(A)** SEM image of a bilayered electrospun vascular graft. Scale bar = 500 μm. SEM images of **(B)** PLLA microfibers on the inner surface and **(C)** PLCG + PCL nanofibers on the outer surface of the graft. Scale bars = 50 μm. **(D)** Representative stress–strain curves of a bilayered vascular graft and a native CCA. **(E)** Average elastic modulus of rat CCA and bilayered vascular grafts ($n = 6$). PLCG, poly(L-lactide-co-caprolactone-co-glycolide); PLLA, poly(L-lactide); PCL, poly(ε-caprolactone); SEM, scanning electron microscope; CCA, common carotid artery.

(Fig. 2C). Mucin concentrations were increased for both passive adsorption and conjugation schemes until a saturation point was reached based on the Alcian blue binding assay. This saturation corresponded to a mucin solution of 0.1% (w/v) for both schemes (data not shown). According to the Alcian blue binding assay, despite using a saturated concentration, more mucin was adsorbed than conjugated to the same type of surface (Fig. 2C).

Release of mucin under static and flow conditions

The stability of mucin on the luminal surface is critical, as unwanted release may increase the likelihood of an immune response, thrombogenesis on the surface or in the blood, and ultimate graft occlusion and failure. To determine the stability of immobilized mucin under a static and hemodynamic environment, we examined mucin release under both static and flow conditions. After a 48-h incubation at 37°C, in the absence or presence of flow, the quantity of mucin adsorbed to the PLLA microfibrous membranes decreased significantly, but some still remained. On the other hand, mucin conjugated to PLLA remained stably attached (Fig. 2C). Although the quantity of mucin remained higher on the adsorbed membranes after 48 h, the difference was not statistically significant.

Anticoagulant activity of mucin

To determine whether mucin had any anticoagulant ability, the effects of mucin, di-amino-PEG (negative control), and heparin (positive control) on coagulation time were measured. Increasing concentrations of mucin in PBS correlated with an increase in rat blood coagulation time, although not as strongly as the increase of heparin concentrations. Di-amino-PEG solution showed a much lower anticoagulant activity than both mucin and heparin (Fig. 3A). The anticoagulant activity of mucin peaked at 1 mg/mL or 0.1% (w/v), which correlated to the mucin concentration that saturated the surface of scaffolds as previously established using the Alcian blue binding assay.

Mucin-modified scaffolds significantly reduced the adhesion of platelets

To determine the effect of mucin modification on platelet adhesion, untreated, PEGylated, PEG-MUC, and MUC membranes were incubated with rat whole blood. Mucin modification significantly decreased the ability of rat platelets to adhere to the membranes (Fig. 3B–F and Supplementary Fig. S1; Supplementary Data are available online at www.liebertpub.com/tea). Additionally, PEGylated membranes showed reduced platelet adhesion as expected (Fig. 3C, F and Supplementary Fig. S1B, F). Statistically, modification with PEG alone, as well as in combination with mucin showed the best ability to prevent platelet adhesion. Such a reduction could aid in the success of graft scaffolds modified by PEG, mucin, or both by preventing platelet adhesion/activation and subsequent thrombus-related failure.

Figure 3B–E show representative SEM images of platelets on untreated, PEGylated, PEG-MUC, and MUC PLLA microfibrous membranes, respectively. It is evident that more activated platelets, as seen by their spiky protrusions, were present on and within the untreated membranes. We also observed the presence of red blood cells on and in the membranes. Other types of blood cells were likely washed away before sample preparation for SEM and immunofluorescent staining.

Mucin-conjugated grafts significantly improved patency rates in vivo

The patency for untreated, PEGylated, MUC, and PEG-MUC bilayered grafts was determined at 1 month postimplantation in the carotid artery. After 1 month implantation in athymic rats, four out of eight (50%) untreated grafts, four out of eight (50%) PEGylated grafts, four out of eight (50%) MUC grafts, and eight out of eight (100%) PEG-MUC grafts were patent, indicating that covalently immobilized mucin, but not adsorbed mucin, significantly improved the patency of vascular grafts.

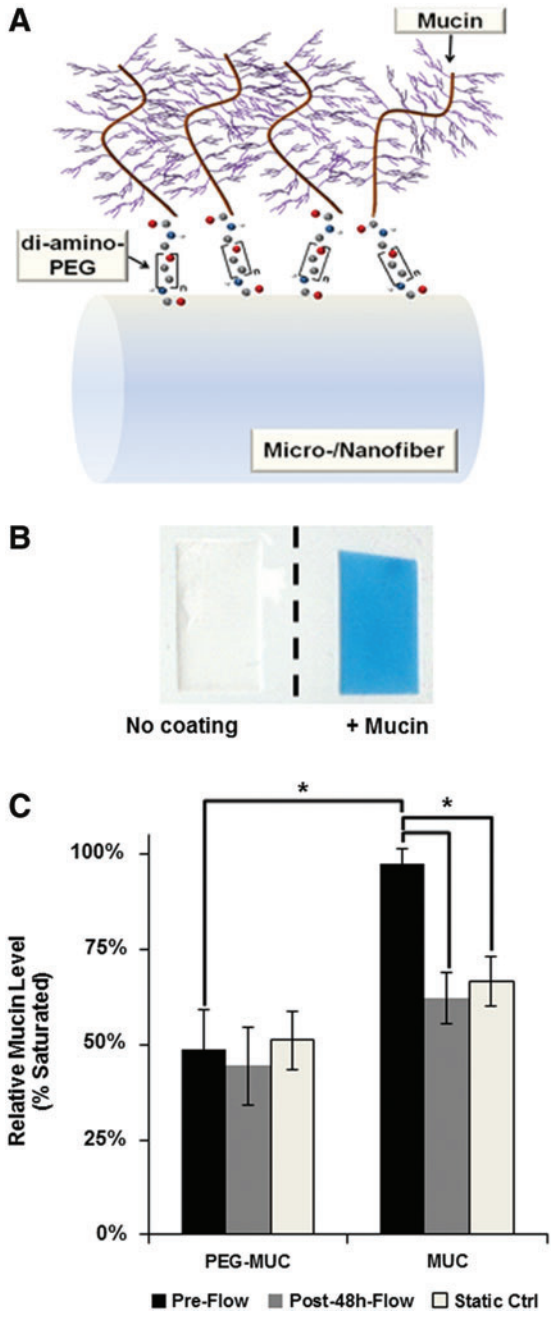

FIG. 2. Mucin immobilization and stability. **(A)** Schematic of mucin conjugation to a fiber using the PEG linker. **(B)** Mucin was conjugated (or adsorbed; not shown) to fibrous scaffolds and incubated with Alcian blue solution, exhibiting blue color. **(C)** PLLA membranes with conjugated or adsorbed mucin were incubated for 48 h at 37°C under static or flow conditions, and the amount of mucin remaining on the membranes was quantified. *$p < 0.05$ based on the Holm's *t*-test, $n = 3$. PEG, di-amino-poly(ethylene glycol). Color images available online at www.liebertpub.com/tea

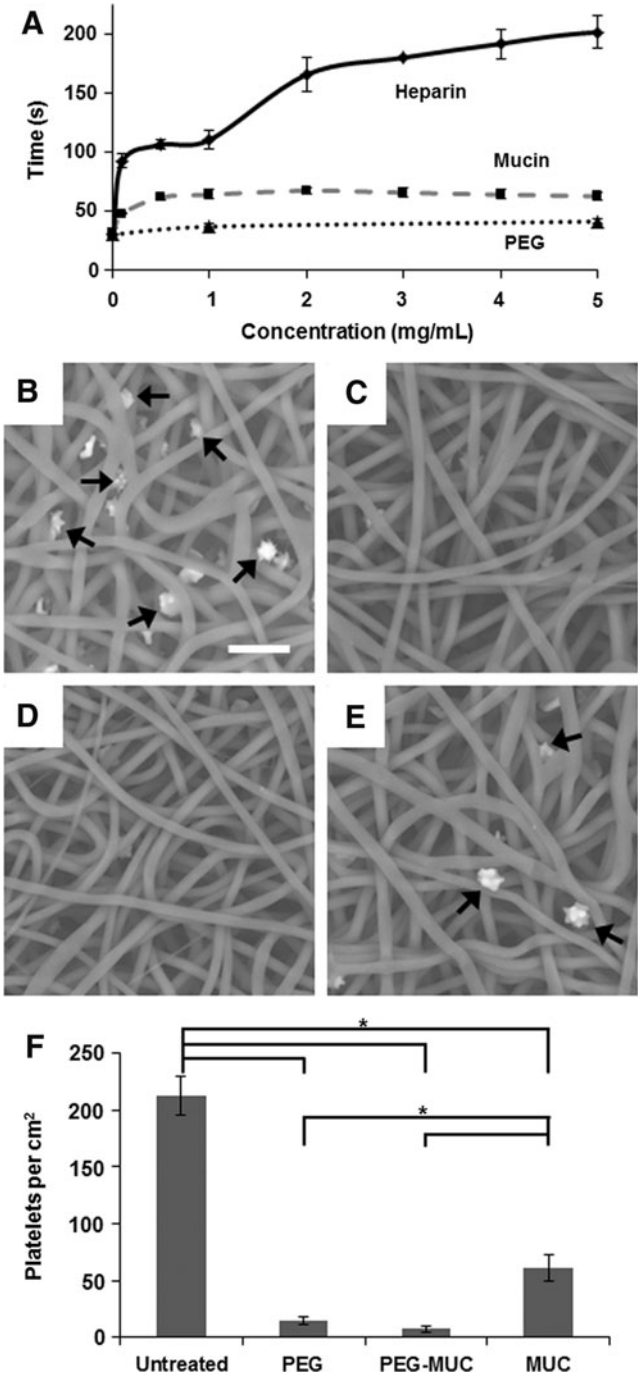

FIG. 3. Effects of mucin on coagulation and platelet adhesion. **(A)** Anticoagulant activity of mucin, heparin (positive control), and PEG (negative control) in phosphate-buffered saline. Coagulation time of whole blood at each concentration of mucin, heparin, and PEG was measured ($n = 3$). Representative SEM images of platelets adhered to **(B)** untreated, **(C)** PEGylated (PEG), **(D)** mucin-conjugated (PEG-MUC), and **(E)** mucin-adsorbed (MUC) PLLA scaffolds. Scale bar = 10 μm. **(F)** Statistical analysis of surface modification effects on platelet adhesion. *$p < 0.05$ based on the Holm's *t*-test, $n = 3$ (9 fields were counted for each sample).

Bilayered graft maintained mechanical strength after 1 month in vivo

To determine whether the mechanical strength of our modified grafts was affected *in vivo*, we performed mechanical tests on rings of the explanted grafts and compared

their average elastic moduli to each other, as well as to the average elastic modulus of preimplanted grafts. As mentioned previously, the elastic modulus of the grafts before implantation was about 12.8 ± 2.5 MPa. After 1 month, the elastic moduli of implanted grafts were 11.3 ± 0.7 MPa (untreated), 12.4 ± 0.3 MPa (PEG), 13.1 ± 0.6 MPa (PEG-MUC), and 12.3 ± 0.8 MPa (MUC). There was no statistical difference in the average elastic modulus between each treatment group at 1 month postimplantation.

Neotissue formation and cell infiltration

The patent grafts of the four groups (untreated, PEGylated, PEG-MUC, and MUC) showed similar histological

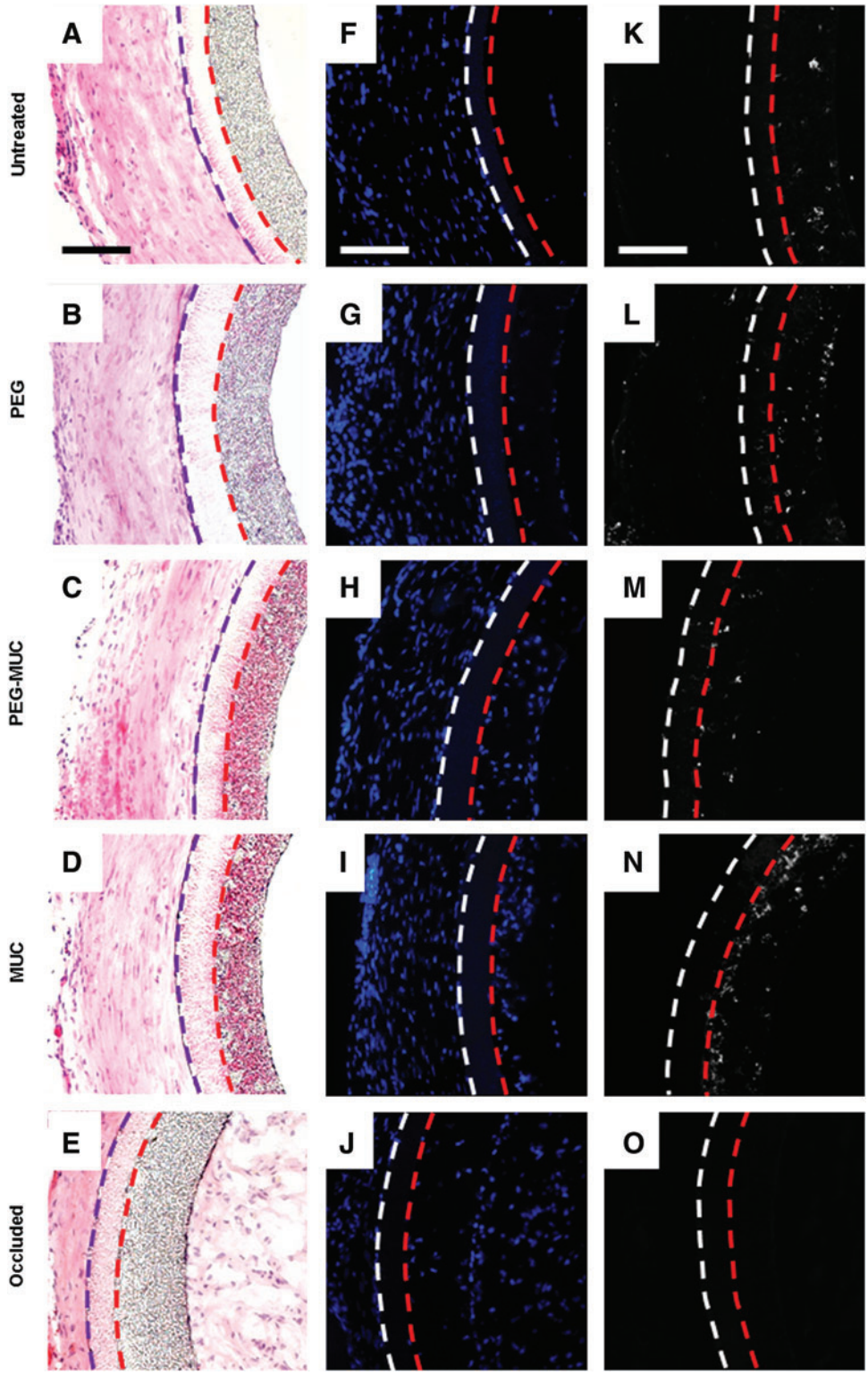

FIG. 4. Cross sections of the explanted grafts at 1 month postimplantation. **(A–E)** Hematoxylin and eosin staining. **(F–J)** DAPI staining. **(K–O)** CD68 staining. Purple or white dotted lines indicate neotissue/PLCG + PCL border. Red dotted lines indicate PLCG + PCL/PLLA border. In all images, right side = luminal side. All scale bars = 100 μm. Color images available online at www.liebertpub.com/tea

characteristics. For the patent grafts, little thrombosis and/or intimal hyperplasia was observed in the middle of the grafts or at the anastomotic sites in each experimental group after 1 month (Fig. 4). The H&E stain indicated that neotissues formed around all the vascular grafts (Fig. 4A–D). Some matrix deposition occurred within the PLLA layer of PEG-MUC and MUC grafts (Fig. 4C, D). Occluded grafts failed due to thrombus formation. An occluded graft (untreated) is exemplified in Figure 4E, showing many cells in the loose matrix (possibly fibrin) inside the occluded lumen.

To clearly show cell distribution in the grafts, cell nuclei were stained by DAPI (Fig. 4F–J). Cell infiltration had occurred by 1 month, but to different extents in each experimental group and was limited to the luminal (i.e., PLLA) layer. PEG-MUC grafts promoted the most cell infiltration. MUC grafts promoted some cell infiltration, but not as much as PEG-MUC grafts. PEGylated grafts had a small amount of cell infiltration, while untreated grafts showed little to none. The extent of cell infiltration correlated well with the amount of matrix deposition in the luminal layers (Fig. 4A–D). CD68 staining revealed a mild presence of macrophages in the luminal layer of all grafts (Fig. 4I–L). M1 and M2 macrophages were not present in the grafts after 1 month, as evidenced by negative staining for CCR7 and CD163, respectively (data not shown). The Ki67 staining of all tissue sections was negative (data not shown), demonstrating that the cells present within the graft walls at 1 month were not proliferative.

Endothelialization and SMC organization

After 1 month, continuous endothelialization was observed on the luminal surface of the patent grafts from all four groups (Fig. 5A–D). Except for the thrombus formation in occluded grafts, little neointima on the luminal surface was observed, and endothelialization was found in all patent grafts around the anastomotic sites (Supplementary Fig. S2). The SM-MHC staining showed that SMCs were the major cell type in neotissues around the grafts (Fig. 5F–I). In contrast, occluded grafts did not have well-organized ECs and SMCs (Fig. 5E, J). These grafts lacked continuous endothelialization on the luminal surface due to the thrombus formation on the luminal surface (Fig. 5E), and some ECs and SMCs were found in the loose matrix inside the occluded lumen (Fig. 5E, J).

Discussion

In this study, we developed a bilayered, electrospun small-diameter vascular scaffold that exhibited excellent performance when chemically modified with mucin. These modified acellular grafts showed a superior patency rate after 1 month *in vivo*. In addition, our graft design, which incorporated two different polymer compositions into the bilayered structure, resulted in the same mechanical property as native arteries. This minimized the mechanical mismatch that could result in the different extent of artery and graft deformation, alter the local hemodynamics, and cause endothelial dysfunction,[42,43] subsequent thrombosis and neointimal hyperplasia, and eventual long-term instability of the grafts. Indeed, little neointima formation was detected around the anastomotic site and endothelialization was achieved (Supplementary Fig. S2).

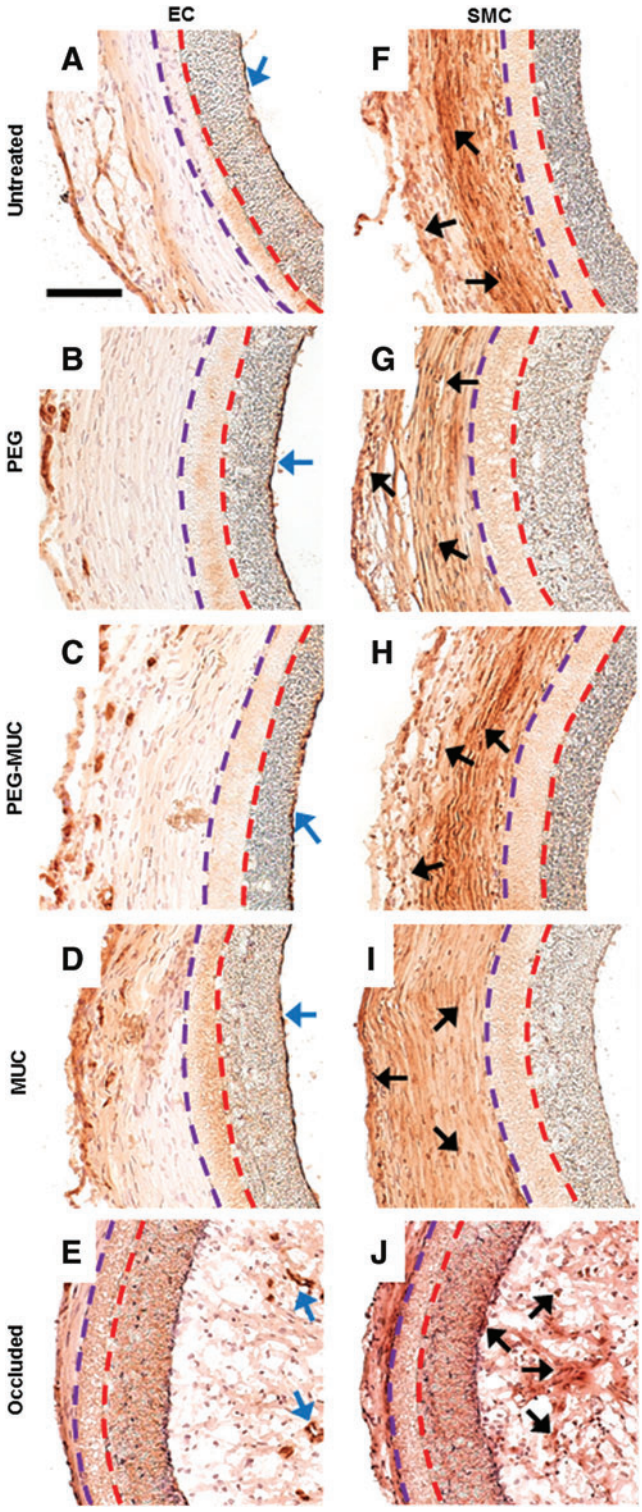

FIG. 5. EC and SMC organization in the explanted grafts at 1 month postimplantation. **(A–E)** CD31 staining (dark brown) for ECs. Blue arrows indicate EC presence on the luminal side. **(F–J)** SM-MHC staining (dark brown) for SMCs. Black arrows exemplified SMC staining. Purple dotted lines indicate neotissue/PLCG+PCL border. Red dotted lines indicate PLCG+PCL/PLLA border. In all images, right side = luminal side. Scale bar = 100 μm. EC, endothelial cell; SMCs, smooth muscle cells; MHC, myosin heavy chain. Color images available online at www.liebertpub.com/tea

A major finding is that covalently bonded mucin, but not adsorbed mucin, can prevent thrombosis and graft occlusion. *In vitro* assessment suggested that this protective activity, at least in part, could be attributed to the ability of mucin to suppress platelet adhesion. The excellent patency of PEG-MUC grafts may be also related to the inhibitory effect of PEG on platelet adhesion. However, the fact that PEGylated grafts did not show as good a patency rate as PEG-mucin grafts suggests other factors contributed to this success *in vivo*. For example, mucin also has a weak anticoagulant activity. In addition, mucin is negatively charged and forms a glycocalyx-like brush layer that could resist the nonspecific adsorption of proteins and the adhesion of blood cells. The latter may especially apply to platelets, whose inherent negative charge may cause them to be repelled from mucin-treated surfaces. The mere presence of mucin by adsorption, however, was insufficient to suppress thrombosis and maintain the patency of grafts *in vivo*. One explanation is that adsorbed mucin is not stable and may detach easily, especially under flow conditions; furthermore, the detached mucin, if forming aggregates, can cause thrombus formation.

Additionally, mucin appeared to increase cell infiltration into the PLLA layer of the graft. This event might be explained by the hydrophilic and negatively charged properties of mucin on the microfibers. It is possible that the negative charge of mucin attracts more water into the scaffold, which consequently increases the porosity of the scaffold for cell infiltration. However, there was no cell infiltration in the much denser outer layer of the vascular grafts, and well-organized SMC layers formed on the outer surface of the grafts. The cells that infiltrated into the PLLA layer included a mild population of macrophages that likely came from circulation. The inflammatory response may have also promoted infiltration of other cell types (e.g., endothelial progenitor cells) into the wall, but did not seem to be a consistent factor contributing to graft failure. With good endothelialization, SMC recruitment, and promotion of cell infiltration, one might design vascular grafts that match the mechanical property of native arteries for the long-term integration into vascular tissues.

Our study described here may serve as a basis for designing an ideal vascular graft. All polymers used for the grafts are biodegradable. However, their degradation rates are slow and may be longer than necessary to support vascular remodeling. Furthermore, the specific amount and orientation of mucin bound to the polymer surfaces need further characterization. As our main goals were to demonstrate the ability to construct a mechanically mimicking conduit and bind mucin to this conduit to increase its hemocompatibility, future studies may be done to optimize polymer composition and employment of mucin on blood-contacting devices.

Conclusions

The use of synthetic, biocompatible materials such as PLLA and PLCG+PCL to produce micro/nanofibrous scaffolds with the mechanical property identical to native arteries demonstrated the feasibility to fabricate mechanically-matched grafts. Mucin can prevent platelet adhesion and has a weak anticoagulant activity. Covalently bonded mucin, but not adsorbed mucin, results in an excellent patency rate. Mucin coating also increased cell infiltration into microfibrous grafts. Mucin-conjugated electrospun vascular grafts may provide a superior off-the-shelf option for small-diameter bypass grafts.

Acknowledgments

This work was supported, in part, by the National Institutes of Health Grants HL 083900 and EB012240 (to S.L.), a Training Grant GM56847 from the National Institute of General Medicine Sciences—Initiative for Maximizing Student Development (NIGMS-IMSD) (to R.R.R.J.), and a Predoctoral Fellowship from the American Heart Association (to Y.Z.).

Disclosure Statement

No competing financial interests exist.

References

1. Nerem, R.M., and Seliktar, D. Vascular tissue engineering. Annu Rev Biomed Eng **3,** 225, 2001.
2. Niklason, L.E., Gao, J., Abbott, W.M., Hirschi, K.K., Houser, S., Marini, R., *et al.* Functional arteries grown *in vitro*. Science **284,** 489, 1999.
3. Weinberg, C.B., and Bell, E. A blood vessel model constructed from collagen and cultured vascular cells. Science **231,** 397, 1986.
4. L'Heureux, N., Dusserre, N., Konig, G., Victor, B., Keire, P., Wight, T.N., *et al.* Human tissue-engineered blood vessels for adult arterial revascularization. Nat Med **12,** 361, 2006.
5. Brennan, M.P., Dardik, A., Hibino, N., Roh, J.D., Nelson, G.N., Papademitris, X., *et al.* Tissue-engineered vascular grafts demonstrate evidence of growth and development when implanted in a juvenile animal model. Ann Surg **248,** 370, 2008.
6. Gong, Z., and Niklason, L.E. Small-diameter human vessel wall engineered from bone marrow-derived mesenchymal stem cells (hMSCs). FASEB J **22,** 1635, 2008.
7. Hashi, C.K., Zhu, Y., Yang, G.Y., Young, W.L., Hsiao, B.S., Wang, K., *et al.* Antithrombogenic property of bone marrow mesenchymal stem cells in nanofibrous vascular grafts. Proc Natl Acad Sci U S A **104,** 11915, 2007.
8. Clowes, A.W., Kirkman, T.R., and Reidy, M.A. Mechanisms of arterial graft healing. Rapid transmural capillary ingrowth provides a source of intimal endothelium and smooth muscle in porous PTFE prostheses. Am J Pathol **123,** 220, 1986.
9. Huynh, T., Abraham, G., Murray, J., Brockbank, K., Hagen, P.O., and Sullivan, S. Remodeling of an acellular collagen graft into a physiologically responsive neovessel. Nat Biotechnol **17,** 1083, 1999.
10. Isenberg, B.C., Williams, C., and Tranquillo, R.T. Small-diameter artificial arteries engineered *in vitro*. Circ Res **98,** 25, 2006.
11. Jordan, S.W., Haller, C.A., Sallach, R.E., Apkarian, R.P., Hanson, S.R., and Chaikof, E.L. The effect of a recombinant elastin-mimetic coating of an ePTFE prosthesis on acute thrombogenicity in a baboon arteriovenous shunt. Biomaterials **28,** 1191, 2007.
12. Hashi, C.K., Derugin, N., Janairo, R.R., Lee, R., Schultz, D., Lotz, J., *et al.* Antithrombogenic modification of small-diameter microfibrous vascular grafts. Arterioscler Thromb Vasc Biol **30,** 1621, 2010.
13. Conklin, B.S., Richter, E.R., Kreutziger, K.L., Zhong, D.S., and Chen, C. Development and evaluation of a novel decellularized vascular xenograft. Med Eng Phys **24,** 173, 2002.

14. Tamura, N., Nakamura, T., Terai, H., Iwakura, A., Nomura, S., Shimizu, Y., *et al.* A new acellular vascular prosthesis as a scaffold for host tissue regeneration. Int J Artif Organs **26,** 783, 2003.
15. Stitzel, J., Liu, J., Lee, S.J., Komura, M., Berry, J., Soker, S., *et al.* Controlled fabrication of a biological vascular substitute. Biomaterials **27,** 1088, 2006.
16. El-Kurdi, M.S., Hong, Y., Stankus, J.J., Soletti, L., Wagner, W.R., and Vorp, D.A. Transient elastic support for vein grafts using a constricting microfibrillar polymer wrap. Biomaterials **29,** 3213, 2008.
17. Soffer, L., Wang, X., Zhang, X., Kluge, J., Dorfmann, L., Kaplan, D.L., *et al.* Silk-based electrospun tubular scaffolds for tissue-engineered vascular grafts. J Biomater Sci Polym Ed **19,** 653, 2008.
18. Nieponice, A., Soletti, L., Guan, J., Deasy, B.M., Huard, J., Wagner, W.R., *et al.* Development of a tissue-engineered vascular graft combining a biodegradable scaffold, muscle-derived stem cells and a rotational vacuum seeding technique. Biomaterials **29,** 825, 2008.
19. Boland, E.D., Matthews, J.A., Pawlowski, K.J., Simpson, D.G., Wnek, G.E., and Bowlin, G.L. Electrospinning collagen and elastin: preliminary vascular tissue engineering. Front Biosci **9,** 1422, 2004.
20. Begovac, P.C., Thomson, R.C., Fisher, J.L., Hughson, A., and Gallhagen, A. Improvements in GORE-TEX vascular graft performance by Carmeda BioActive surface heparin immobilization. Eur J Vasc Endovasc Surg **25,** 432, 2003.
21. Gosselin, C., Vorp, D.A., Warty, V., Severyn, D.A., Dick, E.K., Borovetz, H.S., *et al.* ePTFE coating with fibrin glue, FGF-1, and heparin: effect on retention of seeded endothelial cells. J Surg Res **60,** 327, 1996.
22. Walpoth, B.H., Rogulenko, R., Tikhvinskaia, E., Gogolewski, S., Schaffner, T., Hess, O.M., *et al.* Improvement of patency rate in heparin-coated small synthetic vascular grafts. Circulation **98,** II319; discussion II24, 1998.
23. Wang, X.N., Chen, C.Z., Yang, M., and Gu, Y.J. Implantation of decellularized small-caliber vascular xenografts with and without surface heparin treatment. Artif Organs **31,** 99, 2007.
24. Yu, J., Wang, A., Tang, Z., Henry, J., Li-Ping Lee, B., Zhu, Y., *et al.* The effect of stromal cell-derived factor-1alpha/heparin coating of biodegradable vascular grafts on the recruitment of both endothelial and smooth muscle progenitor cells for accelerated regeneration. Biomaterials **33,** 8062, 2012.
25. Vink, H., and Duling, B.R. Identification of distinct luminal domains for macromolecules, erythrocytes, and leukocytes within mammalian capillaries. Circ Res **79,** 581, 1996.
26. Constantinescu, A.A., Vink, H., and Spaan, J.A. Endothelial cell glycocalyx modulates immobilization of leukocytes at the endothelial surface. Arterioscler Thromb Vasc Biol **23,** 1541, 2003.
27. Simionescu, M., and Simionescu, N. Functions of the endothelial cell surface. Annu Rev Physiol **48,** 279, 1986.
28. Silvestro, L., Ruikun, C., Sommer, F., Duc, T.M., Biancone, L., Montrucchio, G., *et al.* Platelet-activating factor-induced endothelial cell expression of adhesion molecules and modulation of surface glycocalyx, evaluated by electron spectroscopy chemical analysis. Semin Thromb Hemost **20,** 214, 1994.
29. Hollingsworth, M.A., and Swanson, B.J. Mucins in cancer: protection and control of the cell surface. Nat Rev Cancer **4,** 45, 2004.
30. Bansil, R., and Turner, B.S. Mucin structure, aggregation, physiological functions, and biomedical applications. Curr Opin in Colloid Interface Sci **11,** 164, 2006.
31. Shi, L., and Caldwell, K.D. Mucin Adsorption to Hydrophobic Surfaces. J Colloid Interface Sci **224,** 372, 2000.
32. Sandberg, T., Blom, H., and Caldwell, K.D. Potential use of mucins as biomaterial coatings. I. Fractionation, characterization, and model adsorption of bovine, porcine, and human mucins. J Biomed Mater Res A **91,** 762, 2009.
33. Sandberg, T., Karlsson Ott, M., Carlsson, J., Feiler, A., and Caldwell, K.D. Potential use of mucins as biomaterial coatings. II. Mucin coatings affect the conformation and neutrophil-activating properties of adsorbed host proteins—toward a mucosal mimic. J Biomed Mater Res A **91,** 773, 2009.
34. Sandberg, T., Carlsson, J., and Karlsson Ott, M. Interactions between human neutrophils and mucin-coated surfaces. J Mater Sci Mater Med **20,** 621, 2009.
35. Sandberg, T., Carlsson, J., and Ott, M.K. Mucin coatings suppress neutrophil adhesion to a polymeric model biomaterial. Microsc Res Tech **70,** 864, 2007.
36. Shi, L., Ardehali, R., Caldwell, K.D., and Valint, P. Mucin coating on polymeric material surfaces to suppress bacterial adhesion. Colloids Surf B Biointerfaces **17,** 229, 2000.
37. Kurpinski, K.T., Stephenson, J.T., Janairo, R.R., Lee, H., and Li, S. The effect of fiber alignment and heparin coating on cell infiltration into nanofibrous PLLA scaffolds. Biomaterials **31,** 3536, 2010.
38. Ramus, J. Alcian blue: a quantitative aqueous assay for algal acid and sulfated polysaccharides. J Phycol **13,** 345, 1977.
39. Garcia-Manzano, A., Gonzalez-Llaven, J., Lemini, C., and Rubio-Poo, C. Standardization of rat blood clotting tests with reagents used for humans. Proc West Pharmacol Soc **44,** 153, 2001.
40. Schwartz, R.S., Edelman, E., Virmani, R., Carter, A., Granada, J.F., Kaluza, G.L., *et al.* Drug-eluting stents in preclinical studies: updated consensus recommendations for preclinical evaluation. Circ Cardiovasc Interv **1,** 143, 2008.
41. Patel, S., Kurpinski, K., Quigley, R., Gao, H., Hsiao, B.S., Poo, M.M., *et al.* Bioactive nanofibers: synergistic effects of nanotopography and chemical signaling on cell guidance. Nano Lett **7,** 2122, 2007.
42. Boussel, L., Rayz, V., McCulloch, C., Martin, A., Acevedo-Bolton, G., Lawton, M., *et al.* Aneurysm growth occurs at region of low wall shear stress: patient-specific correlation of hemodynamics and growth in a longitudinal study. Stroke **39,** 2997, 2008.
43. Baek, H., Jayaraman, M.V., Richardson, P.D., and Karniadakis, G.E. Flow instability and wall shear stress variation in intracranial aneurysms. J R Soc Interface **7,** 967, 2010.

Address correspondence to:
Song Li, PhD
Department of Bioengineering
University of California, Berkeley
B108A Stanley Hall
Berkeley, CA 94720-1762

E-mail: song_li@berkeley.edu

Received: January 28, 2013
Accepted: August 7, 2013
Online Publication Date: October 16, 2013